

## Recombinant N-Terminal Slit2 Inhibits TGF- $\beta$ -Induced Fibroblast Activation and Renal Fibrosis

Darren A. Yuen,<sup>\*†‡§</sup> Yi-Wei Huang,<sup>†</sup> Guang-Ying Liu,<sup>†</sup> Sajedabanu Patel,<sup>†</sup> Fei Fang,<sup>||</sup> Joyce Zhou,<sup>||</sup> Kerri Thai,<sup>‡</sup> Ahmad Siddiqi,<sup>‡</sup> Stephen G. Szeto,<sup>‡</sup> Lauren Chan,<sup>‡</sup> Mingliang Lu,<sup>‡</sup> Xiaolin He,<sup>‡</sup> Rohan John,<sup>§||</sup> Richard E. Gilbert,<sup>‡§</sup> James W. Scholey,<sup>§||</sup> and Lisa A. Robinson<sup>\*†§</sup>

<sup>\*</sup>Division of Nephrology, The Hospital for Sick Children, Toronto, Ontario, Canada; <sup>†</sup>Program in Cell Biology, The Hospital for Sick Children Research Institute, Toronto, Ontario, Canada; <sup>‡</sup>Keenan Research Centre of Biomedical Science, St. Michael's Hospital, Toronto, Ontario, Canada; <sup>§</sup>Faculty of Medicine, University of Toronto, Toronto, Ontario, Canada; and <sup>||</sup>Division of Nephrology and <sup>||</sup>Department of Laboratory Medicine and Pathobiology, University Health Network, Toronto, Ontario, Canada

### ABSTRACT

Fibrosis and inflammation are closely intertwined injury pathways present in nearly all forms of CKD for which few safe and effective therapies exist. Slit glycoproteins signaling through Roundabout (Robo) receptors have been described to have anti-inflammatory effects through regulation of leukocyte cytoskeletal organization. Notably, cytoskeletal reorganization is also required for fibroblast responses to TGF- $\beta$ . Here, we examined whether Slit2 also controls TGF- $\beta$ -induced renal fibrosis. In cultured renal fibroblasts, which we found to express Slit2 and Robo-1, the bioactive N-terminal fragment of Slit2 inhibited TGF- $\beta$ -induced collagen synthesis, actin cytoskeletal reorganization, and Smad2/3 transcriptional activity, but the inactive C-terminal fragment of Slit2 did not. In mouse models of postischemic renal fibrosis and obstructive uropathy, treatment with N-terminal Slit2 before or after injury inhibited the development of renal fibrosis and preserved renal function, whereas the C-terminal Slit2 had no effect. Our data suggest that administration of recombinant Slit2 may be a new treatment strategy to arrest chronic injury progression after ischemic and obstructive renal insults by not only attenuating inflammation but also, directly inhibiting renal fibrosis.

*J Am Soc Nephrol* 27: 2609–2615, 2016. doi: 10.1681/ASN.2015040356

In the kidney, fibrosis represents the final common pathway of injury present in nearly all types of CKD. Not surprisingly, fibrosis is a major cause of both CKD and ESRD.<sup>1</sup> The global prevalence of CKD and ESRD has risen alarmingly, with roughly one in ten Americans diagnosed with CKD<sup>2</sup> and >\$40 billion spent annually on ESRD care in the United States alone.<sup>3</sup> Although BP control and renin-angiotensin system blockade reduce progressive renal injury, their effects are incomplete, in part because they do not effectively halt progression of renal fibrosis.<sup>4</sup> New therapies are clearly needed.

TGF- $\beta$  is a critical stimulus for fibrogenesis, activating a number of cell types, including kidney fibroblasts, to secrete collagen and other extracellular matrix proteins.<sup>5,6</sup> Binding of TGF- $\beta$  to its receptor complex results in TGF- $\beta$  receptor-mediated phosphorylation of C-terminal serine residues of intracellular Smad2 and Smad3 proteins.<sup>7</sup> This phosphorylation requires an intact actin cytoskeleton, because either pharmacologic or genetic disruption of the cytoskeleton blocks TGF- $\beta$ -induced Smad2/3 phosphorylation.<sup>8</sup> Phosphorylated Smad2 and Smad3 then associate with

Smad4 and are subsequently imported into the nucleus, where they drive the expression of collagen and other extracellular matrix genes.<sup>7</sup>

Slit2 is member of the Slit family of secreted glycoproteins that were initially described as axonal repellents in the developing central nervous system.<sup>9</sup> Binding of Slit2 to its Roundabout-1 receptor (Robo-1) recruits and activates a number of Slit-Robo guanosine 5'-triphosphatase-activating proteins (srGAPs), which in turn, modulate the activity of Rho family GTPases, such as RhoA, Rac, and Cdc42, leading to cytoskeletal rearrangements that control cell shape and migration.<sup>10</sup> We and others have shown more recently that Slit2 is not just important in development but also, that it is active in the mature organism.<sup>11,12</sup> In particular, a variety of leukocytes express Robo-1.<sup>11–14</sup> By inhibiting actin polymerization and cell polarization, Slit2–Robo-1 signaling inhibits chemotaxis,

Received April 4, 2015. Accepted January 12, 2016.

Published online ahead of print. Publication date available at [www.jasn.org](http://www.jasn.org).

**Correspondence:** Dr. Lisa A. Robinson, The Hospital for Sick Children, 555 University Avenue, Room 5265, Toronto, ON M5G 1X8, Canada. Email: [lisa.robinson@sickkids.ca](mailto:lisa.robinson@sickkids.ca)

Copyright © 2016 by the American Society of Nephrology

adhesion, and transendothelial leukocyte migration.<sup>11–14</sup>

In addition to its role in regulating leukocyte motility, the actin cytoskeleton also regulates fibroblast behavior and in particular, responses to TGF- $\beta$ . To date, no studies have examined the ability of Slit2 to regulate profibrotic TGF- $\beta$  signaling. Here, we report that Slit2 inhibits actin stress fiber formation and TGF- $\beta$ -induced Smad signaling, a key profibrotic pathway that drives collagen production in kidney fibroblasts. We further show that Slit2 reduces kidney fibrosis and preserves renal function in mouse models of postischemic renal fibrosis and obstructive uropathy, illustrating the potential therapeutic benefits of a Slit2-based antifibrotic treatment strategy.

To first establish that renal fibroblasts are capable of responding to Slit2, we examined their expression of Slit2 and its Robo receptors. Using RT-PCR and immunoblotting, we showed that NRK49F renal fibroblasts express Slit2, Robo-1, and Robo-2 but not Robo-3 or Robo-4 mRNA (Figure 1A, Supplemental Figure 1). Because Robo-1 is the most well characterized of the Slit2 receptors, we next tested for Robo-1 at the protein level, showing its presence in whole-cell lysates *via* immunoblotting (Figure 1B). Robo-1 was detected predominantly in the plasma membrane, suggesting that fibroblasts express a pool of Robo-1 receptors that are available to bind Slit2 and transduce intracellular signals (Figure 1C). Using dual immunofluorescence staining, we next confirmed our findings *in vivo*, showing that Robo-1 is expressed in interstitial  $\alpha$ -smooth muscle actin<sup>+</sup> ( $\alpha$ -SMA<sup>+</sup>) fibroblasts in the kidney after ureteral obstruction, a model of progressive renal fibrosis (Figure 1D).

We next examined the effects of Slit2 treatment on TGF- $\beta$ -induced fibroblast [<sup>3</sup>H]-proline incorporation, a sensitive measure of collagen production. We found that bioactive N-terminal fragment of Slit2 (N-Slit2) dose dependently inhibited TGF- $\beta$ -induced collagen synthesis by fibroblasts, regardless of whether given before or after TGF- $\beta$  stimulation (Figure 2A, Supplemental

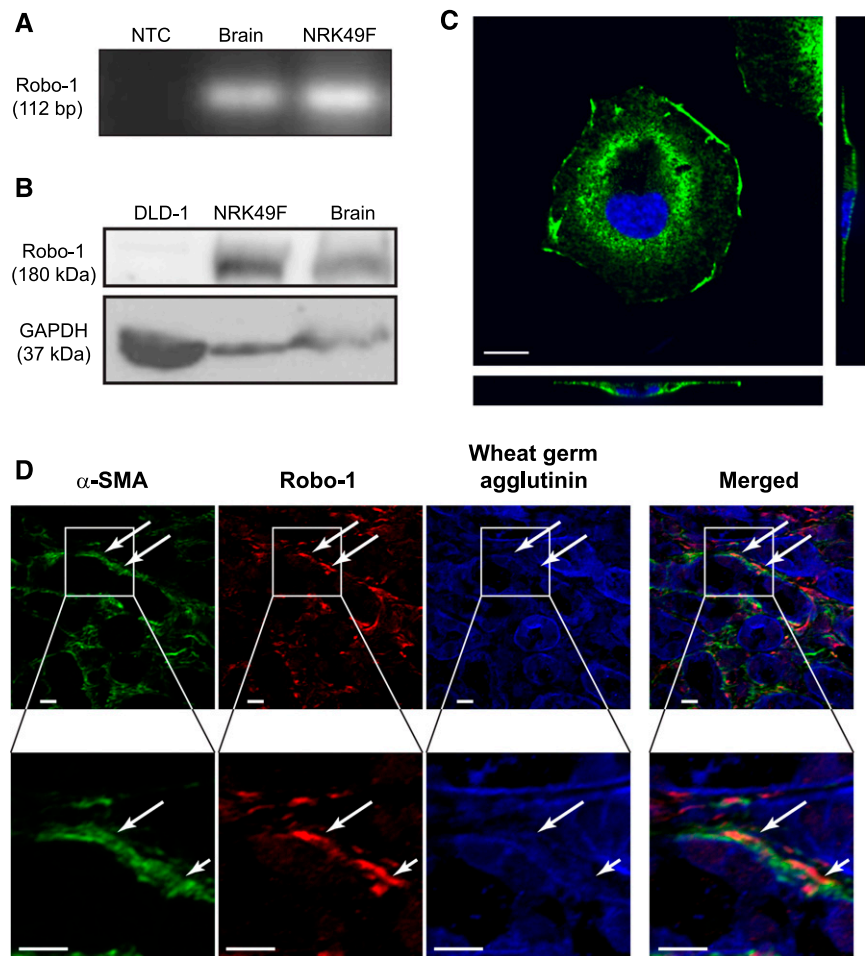


**Figure 1.** Renal fibroblasts express Robo-1. Expression of Robo-1 was assessed in NRK49F fibroblasts using (A) RT-PCR and (B) immunoblotting. In the RT-PCR experiments, no template control (NTC) was used as negative control, and brain tissue was used as positive control. In the immunoblotting experiments, Robo-1-deficient DLD-1 colon epithelial cells were used as negative control,<sup>17</sup> and brain tissue was used as positive control. (C) Immunofluorescence labeling using antibody detecting Robo-1 (green) with 4',6-diamidino-2-phenylindole (DAPI) nuclear counterstaining (blue). Shown are an xy projection (upper left panel), an xz projection (lower panel), and yz projection (right panel) of representative stained cell taken with  $\times 63$  objective. Scale bar, 10  $\mu$ m. (D) Immunofluorescence labeling of fibrotic kidney tissue resected from mouse subjected to UUO. Antibodies detected  $\alpha$ -SMA (green) and Robo-1 (red), with wheat germ agglutinin counterstaining to label cell membranes (blue). Shown is representative image taken with  $\times 40$  objective. Lower panels show magnified view of the regions indicated in upper panels. The white arrows point to green  $\alpha$ -SMA<sup>+</sup> interstitial cells that coexpress Robo-1 (red). Scale bar, 10  $\mu$ m. GAPDH, glyceraldehyde-3-phosphate dehydrogenase.

Figure 2). To confirm the specificity of these observed responses, we preincubated N-Slit2 with molar equivalent amounts of Robo-N, a soluble decoy receptor comprised of the extracellular domain of Robo-1.<sup>15</sup> Neutralization of N-Slit2 with Robo-N effectively abolished the inhibitory effects of N-Slit2 (Figure 2B).

Because an intact and responsive actin cytoskeleton is required for TGF- $\beta$ -induced collagen production by fibroblasts,<sup>8</sup> we next examined the effects of Slit2 on TGF- $\beta$ -induced actin cytoskeletal rearrangements. N-Slit2 significantly blocked TGF- $\beta$ -induced actin stress fiber formation in renal fibroblasts (Figure 2C).

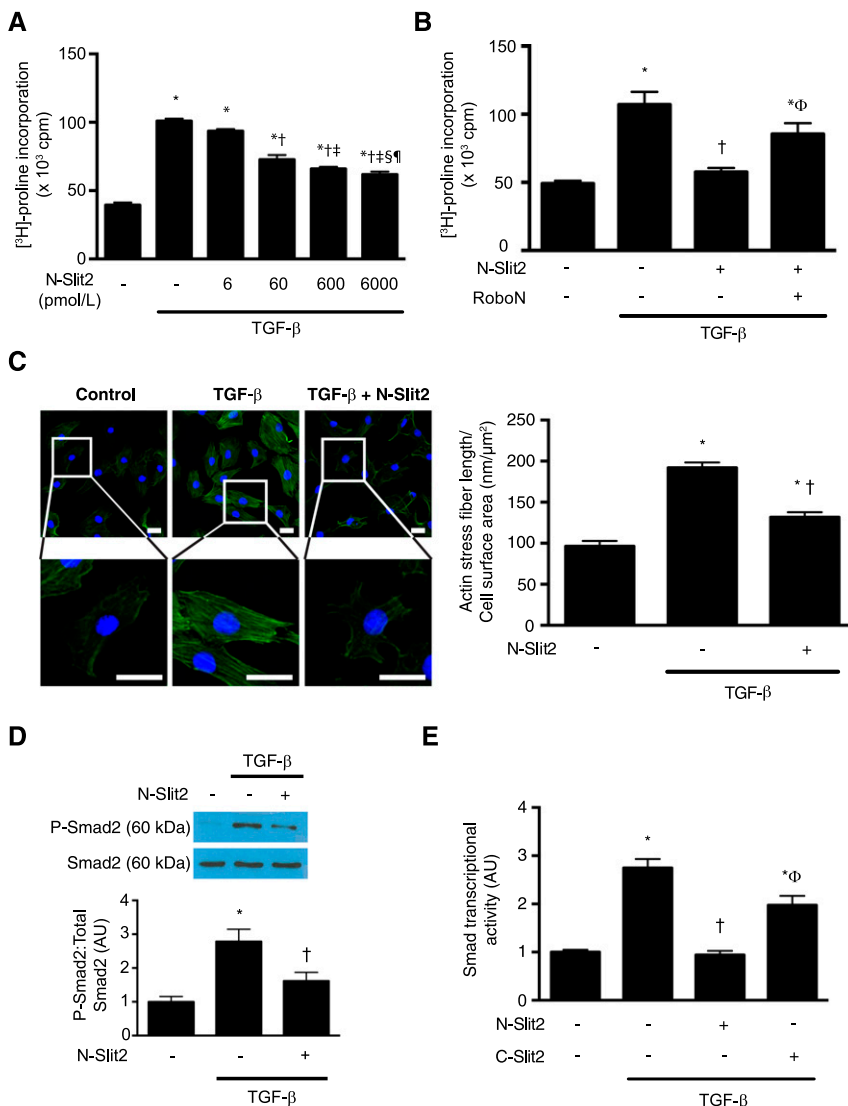


**Figure 2.** Slit2 inhibits TGF- $\beta$ -induced Smad signaling in renal fibroblasts. (A) NRK49F fibroblasts were incubated with TGF- $\beta$  (10 ng/ml) and N-Slit2 at the indicated concentrations. Incorporation of [<sup>3</sup>H]-proline, a marker of collagen production, into protein was measured ( $n=3$ ). (B) Experiments were performed as in A after preincubating N-Slit2 (30 nmol/L) with Robo-N (30 nmol/L;  $n=3$ ). (C) NRK49F cells were incubated with N-Slit2 (30 nmol/L) and then TGF- $\beta$  (10 ng/ml) and labeled with Alexa488-conjugated phalloidin to identify polymerized F-actin (green) and 4',6-diamidino-2-phenylindole (DAPI) to identify nuclei (blue). Representative images are shown from  $n=3$  experiments per condition using  $\times 20$  objective. Total actin stress fiber length was measured and normalized to cell surface area. A minimum of 40 cells per condition was imaged for quantification. Scale bar, 25  $\mu$ m. (D) NRK49F cells were incubated with N-Slit2 (30 nmol/L) for 10 minutes and/or TGF- $\beta$  (10 ng/ml) for 30 minutes. Cells were lysed, and lysates were immunoblotted for phosphorylated Smad2 (P-Smad2) and total Smad2/3. A minimum of 13 replicates was performed per condition. (E) Cells were incubated with N-Slit2 (30 nmol/L), C-Slit2 (30 nmol/L), and/or TGF- $\beta$  (10 ng/ml), and Smad-dependent transcription was measured using a Smad-responsive luciferase reporter system. A minimum of 13 replicates was performed per condition. Means  $\pm$  SEMs. One-way ANOVA with *post hoc* Fisher least significant difference was performed. AU, arbitrary unit; cpm, counts per minute. \* $P<0.05$  versus control; † $P<0.05$  versus TGF- $\beta$ -stimulated cells; ‡ $P<0.05$  versus TGF- $\beta$ - and N-Slit2-treated (6 pmol/L) cells; § $P<0.05$  versus TGF- $\beta$ - and N-Slit2-treated (60 pmol/L) cells; ¶ $P<0.05$  versus TGF- $\beta$ - and N-Slit2-treated (600 pmol/L) cells; Φ $P<0.05$  versus TGF- $\beta$ - and N-Slit2-treated (30 nmol/L) cells.

Given the importance of the Smad2/3 signaling pathway in regulating fibroblast responses to TGF- $\beta$  and the dependence of this pathway on intact actin cytoskeletal responses, we next examined the effects of N-Slit2 on Smad2 phosphorylation and resulting Smad2/3-driven transcriptional activity. Although TGF- $\beta$  stimulated robust Smad2 phosphorylation in NRK49F cells, which are known to express the TGF- $\beta$  receptor complex (Supplemental Figure 3),<sup>16</sup> bioactive N-Slit2 inhibited this Smad2 phosphorylation (Figure 2D), leading to reduced downstream Smad2/3-driven transcription (Figure 2E). An inactive C-terminal fragment of Slit2 (C-Slit2) failed to inhibit TGF- $\beta$ -induced Smad2/3 transcriptional activity (Figure 2E). Furthermore, N-Slit2 treatment of HT29 epithelial cells, which do not express Robo-1,<sup>17</sup> did not inhibit Smad2 phosphorylation induced by TGF- $\beta$  (Supplemental Figure 4). Taken together, these data suggest that Slit2–Robo-1 signaling inhibits collagen production by fibroblasts through inhibition of the TGF- $\beta$  Smad2/3 pathway.

To directly test whether Slit2 can attenuate the development of renal fibrosis *in vivo*, we subjected mice to unilateral ureteral obstruction (UUO), a well established model of progressive renal fibrosis. Mice undergoing UUO surgery were randomized to treatment with control vehicle, active N-Slit2, or inactive C-Slit2, with the first injections beginning immediately before surgery. After 7 days of therapy, despite the presence of tubular damage and inflammation (Supplemental Figure 5), the obstructed kidneys of animals treated with N-Slit2 showed significantly reduced collagen deposition and fewer interstitial cells expressing  $\alpha$ -SMA, a marker of activated myofibroblasts, compared with kidneys from both vehicle- and C-Slit2-treated animals (collagen in Figure 3, A and C and  $\alpha$ -SMA in Figure 3, B and D). Likewise, N-Slit2 treatment significantly reduced mRNA levels of COL3A1 [encoding the  $\alpha$ (1)-chain of type 3 collagen] and ACTA2 (encoding  $\alpha$ -SMA) compared with treatment with either vehicle or C-Slit2

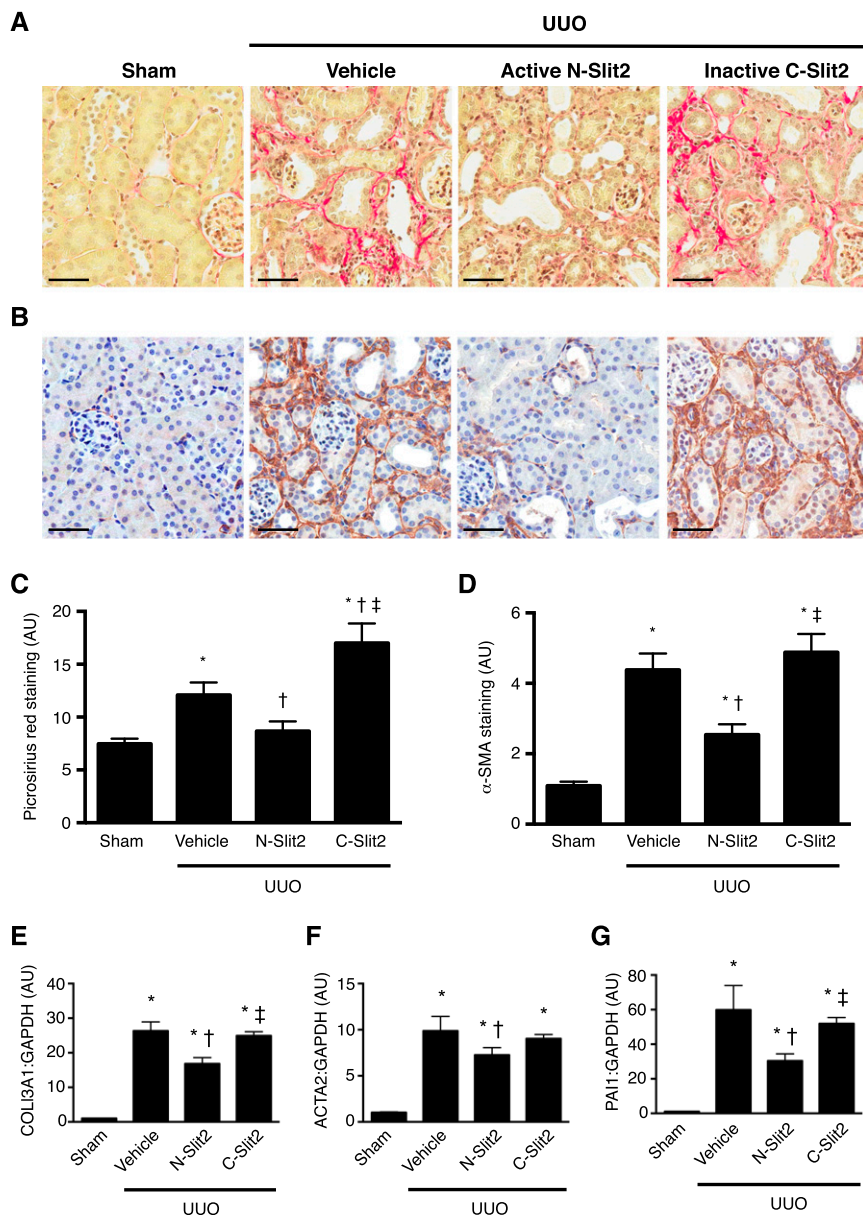


**Figure 3.** Slit2 attenuates renal fibrosis after UUO. Mice were subjected to UUO, and control vehicle ( $n=18$ ), N-Slit2 ( $n=12$ ), or C-Slit2 ( $n=12$ ) was administered as described in Supplemental Material. Sham-operated mice ( $n=12$ ) served as controls. After 7 days, mice were euthanized, and kidney sections were labeled with (A) picrosirius red (PSR) to detect fibrillar collagen or (B) antibody directed to  $\alpha$ -SMA. Representative images were taken with  $\times 16$  objective. Scale bar, 50  $\mu$ m. (C) Experiments were performed as in A, and PSR labeling was digitally quantified. (D) Experiments were performed as in B, and  $\alpha$ -SMA labeling was digitally quantified. (E–G) RNA was isolated from snap-frozen kidney homogenates and after reverse transcription, subjected to quantitative PCR analysis of the profibrotic Smad-inducible genes (E) *COL3A1*, (F) *ACTA2*, and (G) *PAI1*. Means  $\pm$  SEMs. One-way ANOVA with *post hoc* Fisher least significant difference was performed. AU, arbitrary unit; GAPDH, glyceraldehyde-3-phosphate dehydrogenase. \* $P<0.05$  versus sham controls; † $P<0.05$  versus vehicle; ‡ $P<0.05$  versus N-Slit2.

(Figure 3, E and F). In line with our demonstration that N-Slit2 inhibited profibrotic TGF- $\beta$ /Smad signaling in cultured fibroblasts, N-Slit2 treatment

also reduced mRNA levels of plasminogen activator inhibitor-1 (*PAI1*), a well described TGF- $\beta$ /Smad-inducible gene,<sup>18</sup> compared with treatment with

vehicle or C-Slit2 (Figure 3G). These data suggest that bioactive Slit2 can attenuate TGF- $\beta$ -driven renal fibrosis induced by obstructive uropathy.

Although UUO is a well established model of progressive renal fibrosis, the function of the obstructed kidney cannot be easily measured. To examine whether the antifibrotic activity of Slit2 leads to preservation of renal function, we next studied the effects of N-Slit2 on development of fibrosis induced by ischemia-reperfusion injury (IRI), a mouse model of fibrosis that mimics a common form of progressive renal injury in human patients. As was observed in UUO, treatment with N-Slit2 beginning immediately before surgery but not with vehicle or C-Slit2 reduced the deposition of interstitial collagen (Figure 4, A and C) and the number of  $\alpha$ -SMA<sup>+</sup> myofibroblasts (Figure 4, B and D), despite evidence of significant IRI (Supplemental Figure 6). Similarly, N-Slit2 treatment significantly reduced the IRI-induced increase in renal *PAI1* mRNA levels, suggesting that N-Slit2 treatment attenuates profibrotic TGF- $\beta$ /Smad signaling in the injured, ischemic kidney (Supplemental Figure 7).

To assess the effects of Slit2 on kidney function, before study end, all mice underwent nephrectomy of the uninjured right kidney. Twenty-four hours later, blood was collected immediately before euthanasia for measurement of plasma urea and creatinine to assess the function of the injured left kidney. Administration of N-Slit2 led to significant reductions in plasma levels of urea (Figure 4E) and creatinine (Figure 4F). Collectively, these results show that N-Slit2 not only slows the progression of renal fibrosis after ischemic injury but also, improves renal function.

In the above experiments, we initiated Slit2 treatment immediately before either ischemic or obstructive injury. In some clinical settings, such as kidney transplantation, the timing of the insult is known, and thus, a similar preventive regimen could potentially be initiated. In most patients, however, kidney injury is recognized after the causative insult, and treatment is initiated only at this point. We previously showed that N-Slit2

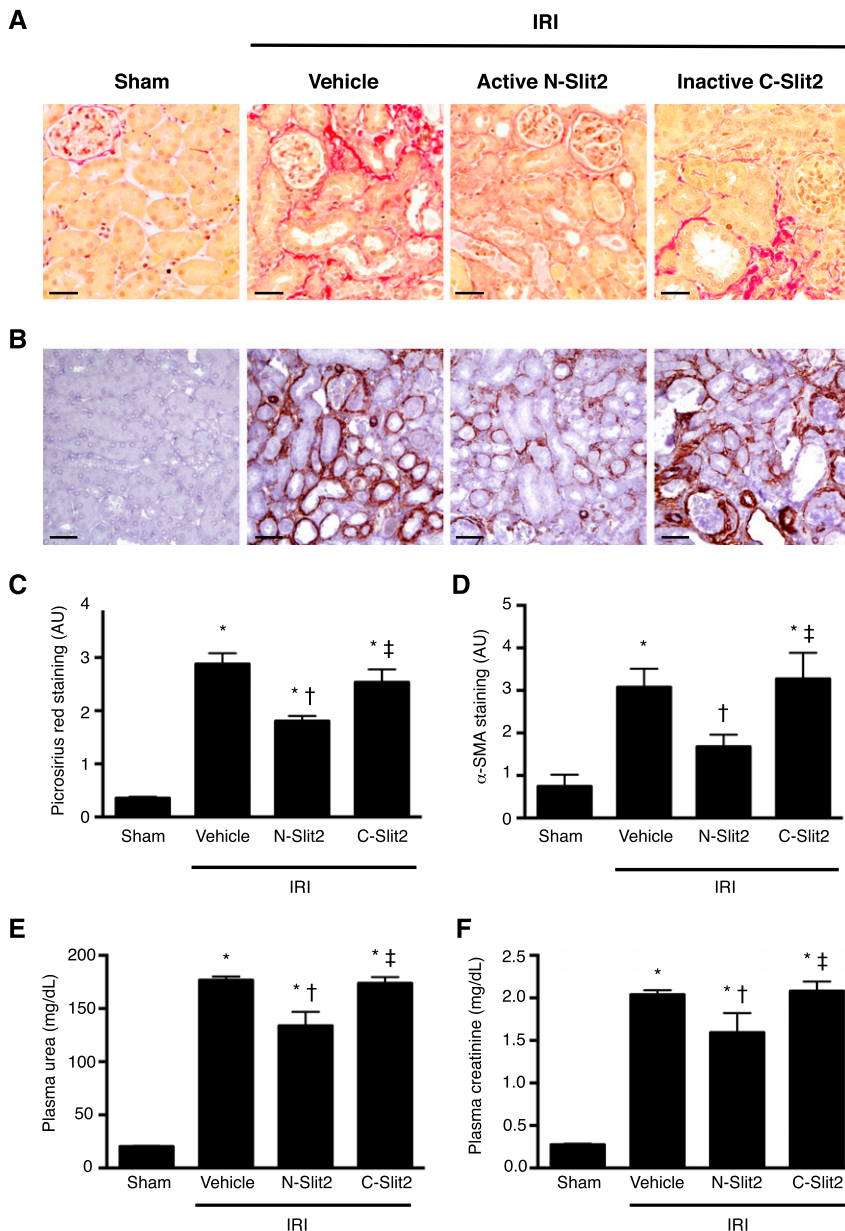


**Figure 4.** Slit2 reduces fibrosis and kidney dysfunction late after IRI. Mice were subjected to renal IRI, and control vehicle ( $n=17$ ), N-Slit2 ( $n=17$ ), or C-Slit2 ( $n=7$ ) was administered as described in Supplemental Material. Sham-operated mice ( $n=6$ ) served as controls. After 14 days, mice were euthanized, and kidney sections were labeled with (A) picrosirius red (PSR) to detect fibrillar collagen or (B) antibody directed to  $\alpha$ -SMA. Representative images were taken with  $\times 16$  objective. Scale bar,  $50\ \mu\text{m}$ . (C) Experiments were performed as in A, and PSR labeling was digitally quantified. (D) Experiments were performed as in B, and  $\alpha$ -SMA labeling was digitally quantified. (E and F) One day before euthanasia, all animals underwent nephrectomy to remove the uninjured right kidney. The next day, blood was collected for measurement of (E) plasma urea and (F) plasma creatinine levels. Means  $\pm$  SEM. One-way ANOVA with *post hoc* Fisher least significant difference was performed. AU, arbitrary unit. \* $P<0.05$  versus sham controls; † $P<0.05$  versus vehicle; ‡ $P<0.05$  versus N-Slit2.

treatment attenuates acute neutrophil infiltration and inflammatory injury in the immediate 24 hours post-renal IRI.<sup>11</sup>

Because inflammation is an important driver of fibrosis, we next tested whether delayed N-Slit2 administration

beginning 72 hours post-IRI would still have renoprotective and antifibrotic effects. At this more clinically relevant time point, the IRI-induced inflammatory response has peaked and is starting to decline,<sup>19,20</sup> whereas fibrogenesis is only beginning.<sup>21</sup> Consistent with the antifibrotic effect that we had observed *in vitro*, delayed administration of N-Slit2 but not C-Slit2 or vehicle reduced renal collagen deposition (Supplemental Figures 8, A and C and 9A) and  $\alpha$ -SMA<sup>+</sup> fibroblast accumulation (Supplemental Figure 8, B and D), despite evidence of significant IRI in the kidney (Supplemental Figure 9B). Importantly, these histomorphometric improvements were associated with an attenuated rise in plasma creatinine, suggesting that delayed N-Slit2 treatment also protects against IRI-induced renal dysfunction (Supplemental Figure 8E).

Our data show that exogenously administered recombinant Slit2 possesses antifibrotic activity *in vitro* and *in vivo* in the kidney after different initial insults. These effects are achieved, at least in part, through the inhibition of TGF- $\beta$ -induced Smad2/3 signaling in renal fibroblasts.

Although myofibroblasts are known to give rise to interstitial fibrotic tissue in the kidney, significant controversy remains as to the predominant precursor cells from which these myofibroblasts originate.<sup>6,22</sup> In this study, we examined the effects of exogenously administered recombinant Slit2 on kidney fibroblasts, because they are a major source of active myofibroblasts in the injured, fibrosing kidney.<sup>22</sup> Although we have shown that Slit2 inhibits the TGF- $\beta$ -induced renal fibroblast-myofibroblast transition, Slit2 may also inhibit the activation of other precursor cell types. For example, a recent study showed that, in the lung, Slit2 prevents recruitment and activation of monocyte-derived fibrocytes, a population of bone marrow-derived cells that can differentiate into active myofibroblasts.<sup>23</sup> Slit2 also prevents chemotactic migration of vascular pericytes, which are other important myofibroblast precursors.<sup>24</sup> Given these reports, future

work will be needed to examine the direct effects of Slit2 on the activation and differentiation of pericytes and bone marrow–derived fibrocytes into activated myofibroblasts in the injured kidney.

After binding its Robo receptors, Slit2 can regulate the activity of Rho family GTPases by activating srGAP proteins. Interestingly, RhoA, a member of the Rho family, is rapidly activated by TGF- $\beta$ , leading to rearrangement of actin monomers into stress fibers, a phenomenon that is required for TGF- $\beta$ –induced Smad activation and collagen transcription.<sup>8</sup> In our study, we observed that renal fibroblasts express both Robo-1 and Robo-2 mRNA, with significant amounts of Robo-1 protein found in the plasma membrane, suggesting the ability of these fibroblasts to respond to Slit2. We further showed that recombinant Slit2 inhibited TGF- $\beta$ –induced actin stress fiber formation. Although our results suggest that Slit2 operates *via* Robo/srGAP-induced inhibition of RhoA, detailed studies are needed to decipher the precise mechanisms underlying the antifibrotic activity of Slit2, including the relative contributions of Robo-1 and Robo-2 to this process.

Despite advances in our understanding of the molecular mechanisms underlying renal fibrosis, no new clinical therapies have been developed over the last four decades. Our findings have exciting translational implications. In particular, a major barrier limiting the pursuit of TGF- $\beta$  neutralizing agents as antifibrotic therapies has been their propensity to exacerbate renal inflammation.<sup>25</sup> Moreover, inflammatory leukocytes in the injured kidney secrete cytokines and growth factors that accelerate fibrogenesis.<sup>26</sup> We and others have previously shown that Slit2 has potent anti-inflammatory effects, diminishing inflammatory cell recruitment by blocking chemoattractant–induced migration, adhesion, and transendothelial leukocyte migration.<sup>11–14</sup> We further showed that Slit2 dramatically reduces inflammation and improves renal

function acutely after renal IRI.<sup>11</sup> Combining its known anti-inflammatory effects with this novel antifibrotic activity, our data suggest the intriguing possibility that exogenously administered Slit2 may be a promising agent to attenuate chronic injury progression after both ischemic and obstructive renal insults.

## CONCISE METHODS

Detailed methods can be found in Supplemental Material.

### Slit2 and Robo-N Purification

A bioactive N-Slit2 and the soluble Slit2 decoy receptor Robo-N were generated as previously described.<sup>11,13,27</sup> A bioinactive C-Slit2 encoding the T1268-S1525 residues of Slit2 was similarly produced.

### Detection of Robo-1

In NRK49F fibroblasts, expression of Slit2, Robo-1, Robo-2, Robo-3, and Robo-4 mRNA was analyzed by RT-PCR. Robo-1 protein was detected *in vitro* and *in vivo* by immunoblotting, and immunofluorescence labeling as per published protocols.<sup>11,13,27</sup>

### In Vitro Slit2 Studies

NRK49F fibroblasts were incubated with N-Slit2 or C-Slit2 followed by TGF- $\beta$ . TGF- $\beta$ –induced [<sup>3</sup>H]–proline incorporation (a measure of collagen production), actin stress fiber formation, Smad2 phosphorylation, and Smad-dependent transcription were then analyzed. In some experiments, N-Slit2 was preincubated with molar equivalent amounts of Robo-N.

### In Vivo Studies

Male C57BL/6 mice underwent left-sided UUO, left-sided unilateral IRI, or sham surgery. Mice undergoing UUO or IRI surgery were randomized to receive injections of normal saline vehicle, N-Slit2, or C-Slit2. Treatment of IRI mice began either before surgery or 72 hours after surgery and continued until study end. Treatment of UUO mice began before surgery and continued until study end. Thirteen days after inducing IRI, mice underwent nephrectomy of the uninjured right kidney. The next day,

blood was collected, and plasma urea and creatinine were measured<sup>19</sup>; 7 days after UUO surgery and 14 days after IRI surgery, mice were euthanized, and the left kidneys were resected.

### Tissue Collection, Preparation, Histology, and Quantitative PCR Studies

Formalin-fixed kidneys were sectioned and incubated with picosirius red, hematoxylin and eosin, periodic acid–Schiff, Masson Trichrome, or an antibody directed to  $\alpha$ -SMA and digitally analyzed.<sup>28–30</sup> Frozen kidney sections were stained with antibodies directed to  $\alpha$ -SMA and Robo-1. RNA was isolated from snap-frozen kidney tissue, and mRNA levels of COL3A1, ACTA2, and/or PAI1 were analyzed by quantitative PCR.

### Statistical Analyses

*P* values were obtained using one-way ANOVA with *post hoc* Fisher least significant difference analysis as appropriate. *P* < 0.05 was deemed significant.

### Study Approval

All animal experiments were approved by The Hospital for Sick Children Animal Care and Use Committee and adhered to the National Institutes of Health Guide for the Care and Use of Laboratory Animals.

## ACKNOWLEDGMENTS

This work was supported by grants from Astellas PharmCanada (to D.A.Y.) and Canadian Institutes of Health Research (CIHR) grant MOP-111083 (to L.A.R.). D.A.Y. was supported by fellowships from the Canadian Society of Transplantation and the CIHR and currently holds Kidney Research Scientist Core Education and National Training Program (KRESCENT) New Investigator Award and Canadian Diabetes Association Clinician Scientist Award. R.E.G. is the Canada Research Chair in Diabetes Complications (Tier 1). J.W.S. was the recipient of CIHR AMGEN Canada Incorporated Chair in Kidney Research. L.A.R. is the Canada Research Chair in Leukocyte Migration in Inflammation and Injury (Tier 2).

## DISCLOSURES

None.

## REFERENCES

- Nath KA: Tubulointerstitial changes as major determinant in the progression of renal damage. *Am J Kidney Dis* 20: 1–17, 1992
- Coresh J, Selvin E, Stevens LA, Manzi J, Kusek JW, Eggers P, Van Lente F, Levey AS: Prevalence of chronic kidney disease in the United States. *JAMA* 298: 2038–2047, 2007
- National Institutes of Health: Kidney Disease Statistics for the United States, Bethesda, MD, National Institutes of Health, 2012
- Debelle FD, Nortier JL, Husson CP, De Prez EG, Vienne AR, Rombaut K, Salmon IJ, Deschodt-Lanckman MM, Vanherweghem JL: The renin-angiotensin system blockade does not prevent renal interstitial fibrosis induced by aristolochic acids. *Kidney Int* 66: 1815–1825, 2004
- Border WA, Noble NA: Transforming growth factor betin tissue fibrosis. *N Engl J Med* 331: 1286–1292, 1994
- Humphreys BD, Lin SL, Kobayashi A, Hudson TE, Nowlin BT, Bonventre JV, Valerius MT, McMahon AP, Duffield JS: Fate tracing reveals the pericyte and not epithelial origin of myofibroblasts in kidney fibrosis. *Am J Pathol* 176: 85–97, 2010
- Attisano L, Wrangé JL: Signal transduction by the TGF- $\beta$  superfamily. *Science* 296: 1646–1647, 2002
- Hubchak SC, Runyan CE, Kreisberg JJ, Schnaper HW: Cytoskeletal rearrangement and signal transduction in TGF- $\beta$ 1-stimulated mesangial cell collagen accumulation. *J Am Soc Nephrol* 14: 1969–1980, 2003
- Brose K, Bland KS, Wang KH, Arnott D, Henzel W, Goodman CS, Tessier-Lavigne M, Kidd T: Slit proteins bind Robo receptors and have an evolutionarily conserved role in repulsive axon guidance. *Cell* 96: 795–806, 1999
- Wong K, Ren XR, Huang YZ, Xie Y, Liu G, Saito H, Tang H, Wen L, Brady-Kalnay SM, Mei L, Wu JY, Xiong WC, Rao Y: Signal transduction in neuronal migration: Roles of GTPase activating proteins and the small GTPase Cdc42 in the Slit-Robo pathway. *Cell* 107: 209–221, 2001
- Chaturvedi S, Yuen DA, Bajw A, Huang YW, Sokollik C, Huang L, Lam GY, Tole S, Liu GY, Pan J, Chan L, Sokolsky Y, Puthi M, Godaly G, John R, Wang C, Lee WL, Brumell JH, Okus MD, Robinson LA: Slit2 prevents neutrophil recruitment and renal ischemia-reperfusion injury. *J Am Soc Nephrol* 24: 1274–1287, 2013
- Wu JY, Feng L, Park HT, Havlioglu N, Wen L, Tang H, Bacon KB, Jiang Zh, Zhang Xc, Rao Y: The neuronal repellent Slit inhibits leukocyte chemotaxis induced by chemotactic factors. *Nature* 410: 948–952, 2001
- Tole S, Mukovozov IM, Huang YW, Magalhaes MA, Yan M, Crow MR, Liu GY, Sun CX, Durocher Y, Glogauer M, Robinson LA: The axonal repellent, Slit2, inhibits directional migration of circulating neutrophils. *J Leukoc Biol* 86: 1403–1415, 2009
- Prasad A, Qamri Z, Wu J, Ganju RK: Slit-2/Robo-1 modulates the CXCL12/CXCR4-induced chemotaxis of T cells. *J Leukoc Biol* 82: 465–476, 2007
- Wu W, Wong K, Chen J, Jiang Z, Dupuis S, Wu JY, Rao Y: Directional guidance of neuronal migration in the olfactory system by the protein Slit. *Nature* 400: 331–336, 1999
- Gaedeke J, Noble NA, Border WA: Curcumin blocks multiple sites of the TGF- $\beta$  signaling cascade in renal cells. *Kidney Int* 66: 112–120, 2004
- Zhou WJ, Geng ZH, Chi S, Zhang W, Niu XF, Lan SJ, M L, Yang X, Wang LJ, Ding YQ, Geng JG: Slit-Robo signaling induces malignant transformation through Hakai-mediated E-cadherin degradation during colorectal epithelial cell carcinogenesis. *Cell Res* 21: 609–626, 2011
- Dennler S, Itoh S, Vivien D, ten Dijke P, Huet S, Gauthier JM: Direct binding of Smad3 and Smad4 to critical TGF  $\beta$ -inducible elements in the promoter of human plasminogen activator inhibitor-type 1 gene. *EMBO J* 17: 3091–3100, 1998
- Li L, Huang L, Vergis AL, Ye H, Bajw A, Narayan V, Strieter RM, Rosin DL, Okus MD: IL-17 produced by neutrophils regulates IFN- $\gamma$ -mediated neutrophil migration in mouse kidney ischemia-reperfusion injury. *J Clin Invest* 120: 331–342, 2010
- Li L, Okus MD: Blocking the immune response in ischemic acute kidney injury: The role of adenosine 2A agonists. *Nat Clin Pract Nephrol* 2: 432–444, 2006
- Furuichi K, Gao JL, Murphy PM: Chemokine receptor CX3CR1 regulates renal interstitial fibrosis after ischemia-reperfusion injury. *Am J Pathol* 169: 372–387, 2006
- LeBleu VS, Taduri G, O'Connell J, Teng Y, Cooke VG, Wod C, Sugimoto H, Kalluri R: Origin and function of myofibroblasts in kidney fibrosis. *Nat Med* 19: 1047–1053, 2013
- Pilling D, Zheng Z, Vakil V, Gomer RH: Fibroblasts secrete Slit2 to inhibit fibrocyte differentiation and fibrosis. *Proc Natl Acad Sci U S A* 111: 18291–18296, 2014
- Guijarro-Muñoz I, Cuest AM, Alvarez-Cienfuegos A, Geng JG, Alvarez-Vallin L, Sanz L: The axonal repellent Slit2 inhibits pericyte migration: Potential implications in angiogenesis. *Exp Cell Res* 318: 371–378, 2012
- Christ M, McCartney-Francis NL, Kulkarni AB, Ward JM, Mizel DE, Mackall CL, Gress RE, Hines KL, Tian H, Karlsson S: Immune dysregulation in TGF- $\beta$ 1-deficient mice. *J Immunol* 153: 1936–1946, 1994
- Lee SB, Kalluri R: Mechanistic connection between inflammation and fibrosis. *Kidney Int Suppl* 119: S22–S26, 2010
- Patel S, Huang YW, Rehman A, Pluthero FG, Chaturvedi S, Mukovozov IM, Tole S, Liu GY, Li L, Durocher Y, Ni H, Kahr WH, Robinson LA: The cell motility modulator Slit2 is potent inhibitor of platelet function. *Circulation* 126: 1385–1395, 2012
- Yuen DA, Connelly KA, Advani A, Liao C, Kuliszewski MA, Trogadis J, Thai K, Advani SL, Zhang Y, Kelly DJ, Leong-Poi H, Keating A, Marsden PA, Stewart DJ, Gilbert RE: Culture-modified bone marrow cells attenuate cardiac and renal injury in chronic kidney disease rat model vinovel antifibrotic mechanism. *PLoS One* 5: e9543, 2010
- Yuen DA, Connelly KA, Zhang Y, Advani SL, Thai K, Kabir G, Kepecs D, Spring C, Smith C, Batruch I, Kosanam H, Advani A, Diamandis E, Marsden PA, Gilbert RE: Early outgrowth cells release soluble endocrine antifibrotic factors that reduce progressive organ fibrosis. *Stem Cells* 31: 2408–2419, 2013
- Yuen DA, Kepecs DM, Zhang Y, Advani S, Thai K, Connelly KA, Gilbert RE: Repeated treatment with bone marrow cell secretory products maintains long-term renoprotection in experimental chronic kidney disease: A placebo-controlled trial. *Can J Kidney Health Dis* 2: 44, 2015

This article contains supplemental material online at <http://jasn.asnjournals.org/lookup/suppl/doi:10.1681/ASN.2015040356/-/DCSupplemental>.